Cell Host & Microbe
Article

ATP-Mediated Erk1/2 Activation Stimulates Bacterial Capture by Filopodia, which Precedes *Shigella* Invasion of Epithelial Cells

Stéphane Romero,[1,2,3] Gianfranco Grompone,[4,5,7] Nathalie Carayol,[1,2,3] Joëlle Mounier,[4,5] Stéphanie Guadagnini,[6] Marie-Christine Prevost,[6] Philippe J. Sansonetti,[4,5] and Guy Tran Van Nhieu[1,2,3,*]
[1]Equipe Communication Intercellulaire et Infections Microbiennes, Centre de Recherche Interdisciplinaire en Biologie, Collège de France, 75005 Paris, France
[2]Institut National de la Santé et de la Recherche Médicale U1050,75005 Paris, France
[3]Centre National de la Recherche Scientifique UMR7241,75005 Paris, France
[4]Institut National de la Santé et de la Recherche Médicale U786, 75015 Paris, France
[5]Unité de Pathogénie Microbienne Moléculaire
[6]Plate-Forme de Microscopie Ultrastructurale
Institut Pasteur, 75015 Paris, France
[7]Present address: Gut Microbiology and Probiotics Facility, Danone Research, 91120 Palaiseau, France, and Institut Pasteur de Montevideo, Mataojo, 11400 Montevideo, Uruguay
*Correspondence: guy.tran-van-nhieu@college-de-france.fr
DOI 10.1016/j.chom.2011.05.005

SUMMARY

***Shigella*, the causative agent of bacillary dysentery in humans, invades epithelial cells, using a type III secretory system (T3SS) to inject bacterial effectors into host cells and remodel the actin cytoskeleton. ATP released through connexin hemichanels on the epithelial membrane stimulates *Shigella* invasion and dissemination in epithelial cells. Here, we show that prior to contact with the cell body, *Shigella* is captured by nanometer-thin micropodial extensions (NMEs) at a distance from the cell surface, in a process involving the T3SS tip complex proteins and stimulated by ATP- and connexin-mediated signaling. Upon bacterial contact, NMEs retract, bringing bacteria in contact with the cell body, where invasion occurs. ATP stimulates Erk1/2 activation, which controls actin retrograde flow in NMEs and their retraction. These findings reveal previously unappreciated facets of interaction of an invasive bacterium with host cells and a prominent role for Erk1/2 in the control of filopodial dynamics.**

INTRODUCTION

Diversion of host cytoskeletal processes is a strategy developed by invasive bacteria to establish and maintain a successful infection (Cossart and Sansonetti, 2004; Ogawa et al., 2008). *Shigella flexneri*, the causative agent of bacillary dysentery, triggers its internalization into epithelial cells through a type III secretion system (T3SS) and elicits an acute inflammatory reaction responsible of the destruction of the colonic epithelium (Phalipon and Sansonetti, 2007). *Shigella* is considered as a potent enteroinvasive bacterium since as little as ten to 100 bacteria are sufficient to cause the disease in humans despite the fact that in vitro bacteria do not adhere to cells. At the basal state, the T3SS is inactive and presents at its tip two type III substrates, IpaB and IpaD, which form a so-called "tip complex" (Veenendaal et al., 2007). The tip complex proteins regulate the activity of the T3SS and could participate in the recognition of host cell receptors, such as β1-integrins or the hyaluronan receptor CD44 (Lafont et al., 2002; Parsot et al., 1995; Veenendaal et al., 2007; Watarai et al., 1997). Upon cell contact, IpaB and IpaC are secreted by the T3SS and insert into the host plasma membrane, forming a so-called "translocator" required for the injection of type III effectors that act in concert to promote bacterial invasion (Galán and Wolf-Watz, 2006; Ogawa et al., 2008).

Recent evidence indicates a role for intercellular signaling mediated by Connexins (Cx) during bacterial infection (Garg et al., 2005; Guttman et al., 2010; Tran Van Nhieu et al., 2003). Cxs are transmembrane proteins that oligomerize in hexamers, or connexons (Willecke et al., 2002). Pairs of connexons from adjacent cells appose to form open channels that are the basis for gap intercellular junctional communication (GIJC). In addition to GIJCs, Cx hexamers can form hemichanels at the plasma membrane that release of ATP or NAD in the extracellular medium (Spray et al., 2006). *Shigella* entry induces calcium transients and ATP-mediated paracrine signaling through the opening of Cx hemichanels, which further stimulates invasion (Tran Van Nhieu et al., 2003; Clair et al., 2008). Here, we investigated the mechanism through which ATP and Cx-mediated signaling stimulate bacterial invasion and dissemination. We show that prior to contact with the cell body, *Shigella* is captured by filopodial extensions, which we termed NMEs for "nanometer-thin micropodial extensions." After bacterial contact, which depends on the T3SS tip complex proteins, NMEs retract, leading to apposition of the bacteria to the cell body and subsequent engulfment. NME-mediated bacterial capture occurs in noncommunicating cells but is stimulated by Cx-mediated signaling and extracellular ATP. We show that NME retraction requires activation of the Erk1/2 MAP kinase. Inhibition of NME

retraction points at a prominent role of these extensions during the initial phases of *Shigella* invasion of epithelial cells.

RESULTS

Bacterial Capture by NMEs Precedes Invasion and Requires the IpaB and IpaD T3SS Components

Because *Shigella* does not express any known adhesin, most studies on bacterial entry were performed via enhancing invasion by centrifugation or using an ectopic adhesin to enhance bacterial contact with host cells. When analyzing the very early stages of cell interaction, we observed that wild-type *Shigella* attached to pre-existing filopodia at the cell periphery (Figure 1A and Movie S1 available online). Bacterial interaction with filopodia represented a major mode of interaction at these early time points since bacteria were seldom found in direct contact with the main cell body (Figure 1A). Despite the fact that a large multiplicity of infection (multiplicity of infection [MOI] = 500 bacteria/cell) was used and many filopodia were present at the cell surface, only a limited fraction of bacterial captures were observed, in addition, bacterial capture occurred essentially via filopodia present at the cell periphery and not by filopodia at the dorsal cell surface (Figure 1A and Figure S1). These observations suggested that only a limited numbers of filopodia have the ability to interact with bacteria. To account for a potential heterogeneity between filopodia, we used the term "NMEs" to describe these extensions. Interaction with NMEs was not observed with BS176, a *Shigella* strain cured from the virulence plasmid, or a *Shigella mxiD* mutant, indicating that a functional T3SS is required for capture (data not shown). Furthermore, capture was inhibited when bacteria were incubated with antibodies directed against the T3SS IpaB or IpaD tip complex proteins (Figure 1B). Scanning electron microscopy analysis showed that NMEs had a diameter of 100–200 nm and a length ranging from 5 to 15 μm (Figure 1C). In a few cases, bacterial interaction was detected with the side of NMEs (Figure S1), but the majority of events occurred between one bacterial pole and a region immediately adjacent to the tip of NMEs (71% ± 4% of total capture events, 98 events scored, n = 6; Figure 1C, top panels), in some instances, establishing a tight apposition (Figure 1C, bottom panels). Bacteria could also be detected contacting these extensions emanating from entry sites (Figure 1D, arrowhead), indicating that NME-mediated capture could occur during the invasion process, possibly increasing the number of bacterial invading at the same site. As expected for filopodia, fluorescence staining indicated that NMEs contained F-actin (Figure S2 and Movie S1).

To circumvent the difficulty of analysis in time-lapse phase-contrast microscopy linked to the swirling of NMEs in 3D and to the low levels of bacterial interaction with cells, we used BS167, a *Shigella galU* mutant (Maurelli et al., 1985). BS167 is deprived of an LPS 0-antigen side chain and shows increased adherence to glass and cells. This property allows reduction of the number of bacteria in the assay to analyze these captures in the focal plane of the coverslip. Time-lapse acquisition indicated that upon bacterial contact, NMEs retracted at an average speed of 5.1 ± 0.5 μm/min (n = 6), pulling the bound bacteria in contact with the main cell body where invasion occurs (Figure 1E). The majority of NME-mediated bacterial capture events was followed by bacterial invasion, with 62% leading to entry foci formation (109 cells, n = 4; Movie S2). When cells were challenged with the noninvasive *Shigella* isogenic plasmid-cured derivative BS169, a 6-fold decrease of the number of capture by NMEs was observed, consistent with the role of IpaB and IpaD. Furthermore, bacterial captures were rarely followed by NME retraction events, and bacteria remained bound at the tip of the NME for extended periods of time, suggesting a role for the T3SS in NME retraction.

Extracellular ATP-Mediated Signaling Amplifies Bacterial Capture by NMEs and Induces Erk1/2 Activation

HeLa cells do not express any known connexins and are deficient for cell-cell communication (Saez et al., 2003). Cx transfectants of HeLa cells are proficient for extracellular ATP-mediated signaling, which increases *Shigella* invasion (Tran Van Nhieu et al., 2003). To test the role of extracellular ATP-mediated signaling in bacterial capture by NME, we performed time-lapse experiments using HeLa cells or HeLa transfectants expressing human connexin 26 (HCx26) challenged with *Shigella*. Two independent clones of HCx26 cells were used, which gave similar results (Experimental Procedures). As shown in Figure 1B, bacterial capture by NMEs was also observed in HCx26 cells, which was inhibited by anti-IpaB or anti-IpaD antibodies, but occurred at a 3.7-fold higher frequency per cell compared to parental HeLa cells. Time-lapse acquisition indicated that the frequency of bacterial capture per cell followed by NME retraction was 3.5-fold higher in HCx26 cells compared to HeLa cells (Figure 2A, solid bars). When ATP was added to HeLa cells during bacterial challenge, the frequency of NME-mediated bacterial captures was increased to levels similar to those observed in HCx26 cells (Figure 2A). Consistent with a role for NME capture in bacterial invasion, during the 30 min duration of these time-lapse acquisitions, the majority (62%–88%) of bacterial capture by NME events led to entry foci formation (Figure 2A, gray bars). Measurements from time lapse acquisitions indicated a similar average speed of retraction of NME after bacterial capture in HeLa (5.1 ± 0.5 μm/min, 25 determinations, n = 6) and HCx26 cells (4.9 ± 0.9 μm/min, 18 determinations, n = 6), indicating that the difference in NME-mediated capture was not linked to increased NME dynamics of retraction.

ATP also induced a transient increase in the tyrosyl-phosphorylation of a 42 kDa band, detected between 2.5 and 10 min after the addition in HeLa cells (Figure 2B, top panel). Probing with an anti-phospho Erk antibody showed that the p42 probably corresponded to the activated form of Erk1/2 (Figure 2B, bottom panel). Wild-type invasive *Shigella* induced a weak activation of Erk1/2 in noncommunicating parental HeLa cells, which was not significantly different than that induced by the *mxiD* mutant (Figure 2C). In contrast, when HCx26 communicating cells were challenged with invasive *Shigella*, a transient activation of Erk1/2 could be clearly detected after the first 5 min of infection, consistent with ATP-mediated signaling in these cells (Figure 2D). These results indicate that bacterial capture is more efficient in Cx-expressing cells proficient for ATP-mediated signaling and that extracellular ATP signaling induces the activation of Erk1/2.

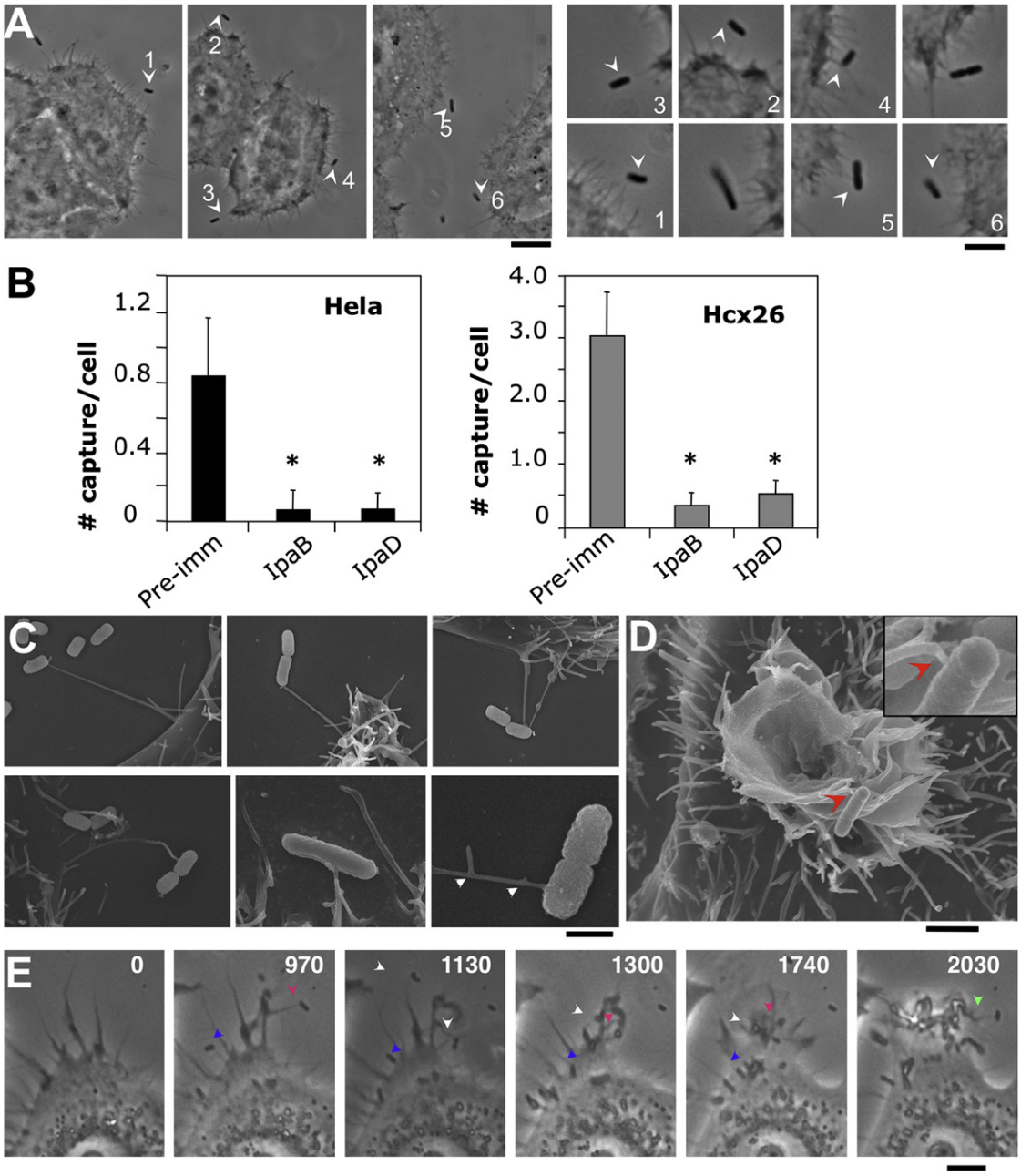

Figure 1. Bacterial Capture by NMEs Precedes *Shigella* Invasion

(A) Representative images of wild-type *Shigella* captured by NMEs. HeLa cells were challenged with wild-type *Shigella* at a MOI of 500 for 15 min at 37°C. Samples were fixed and observed by phase-contrast microscopy. The arrowheads point at individual capture events. Scale bars represent 5 μm.

(B) The T3SS tip complex IpaB and IpaD proteins are required for bacterial capture. Bacteria were incubated with polyclonal anti-IpaB, anti-IpaD, or preimmune serum prior to addition to HeLa cells (left panel) or HCx26 communicating cells (right panels). Anti-IpaB or -IpaD antibodies inhibit NME capture of *Shigella*. Error bars correspond to the standard error of the mean (SEM). n = 3. HeLa, 309 cells; Hcx26, 277 cells. *$p < 0.0001$.

(C and D) Scanning electron microscopy *Shigella* capture by NMEs. Samples were prepared as in (A) and were processed for Scanning electron microscopy analysis (Experimental Procedures). In (C), NMEs are visualized as 50–200 nm thin extensions, sometimes branched (arrowheads). The scale bar represents 1 μm. In (D), bacterial capture is also observed with NMEs emanating from invasion sites (arrowhead). The inset shows a higher magnification of the captured bacteria. The scale bar represents 5 μm.

(E) Time-lapse analysis of bacterial capture by NMEs. HeLa cells were challenged with the invasive BS167 *Shigella* strain (Experimental Procedures) at a MOI of 50. The panels correspond to frames at the time indicated in seconds. Colored arrowheads point at distinct bacterial captures and subsequent NME retraction events. The scale bar represents 5 μm.

See also Figures S1 and S2 and Movies S1 and S2.

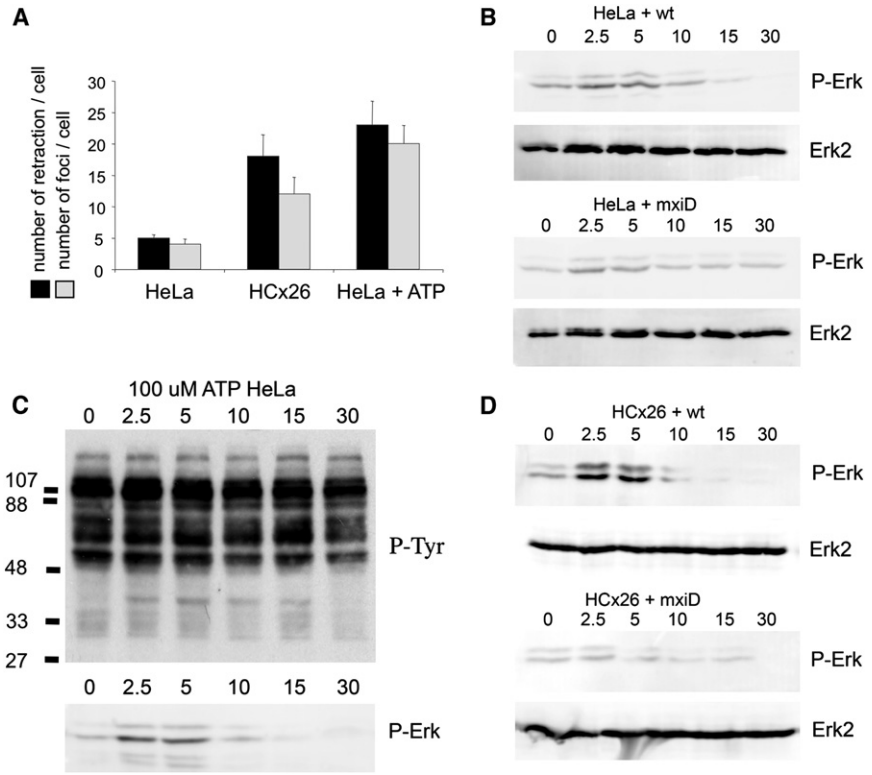

Figure 2. ATP- and Connexin-Mediated Signaling Amplifies Bacterial Capture and Induces Erk1/2 Activation during *Shigella* Invasion

(A) Cells were challenged with the *Shigella* BS167 strain and bacterial capture by NMEs was analyzed by time-lapse phase-contrast microscopy. HeLa, HCx26 cells or HeLa cells challenged in the presence of 50 μM ATP bacterial capture followed by NME retraction (black bars) or bacterial capture and retraction followed by an entry foci formation (gray bars) ± SEM were quantified in at least three independent sets of experiments. (HeLa, 61 cells; HCx26, 54 cells; HeLa + ATP, 72 cells.)

(B) Extracellular ATP stimulates Erk1/2 transient activation. HeLa cells were treated with 100 μM ATP for the indicated times in minutes, and cell lysates were analyzed by western blotting with anti-phosphotyrosine (top) or anti-phosphorylated Erk (bottom) antibodies. The molecular weight markers are indicated.

(C and D) Invasive *Shigella* induces Erk1/2 activation in HCx26 cells. Cells were challenged with bacteria for the indicated times, and samples were lysed and processed for anti-phosphorylated Erk2 (P-Erk2) or anti-Erk2 (Erk2) western blot analysis. Cells challenged with the following: wt, wild-type *Shigella* strain; mxiD, an isogenic T3SS-deficient *mxiD* mutant strain. HeLa cells (C) and HCx26 cells (D) were used. Quantification indicated no statistical difference between the levels of phosphorylated Erk2 induced by wild-type *Shigella* or the *mxiD* mutant in HeLa cells. In contrast, in HCx26 cells, wild-type *Shigella* induced an increase in the intensity of phosphorylated Erk2 signal reaching up to 3.9-fold ± 0.6-fold that observed with the *mxiD* mutant (n = 3). *$p < 0.01$ when tested against samples challenged with the wild-type *Shigella* strain M90T.

Erk1/2 Is Required for NME Retraction

The enhanced Erk1/2 activation observed in HCx26 cells suggested that this kinase could play a role in NME-mediate bacterial capture. To visualize the effect of ATP on Erk1/2 localization, we transfected HeLa cells with GFP-Erk2 and stimulated them with ATP (Experimental Procedures). In the absence of stimulation, Erk2 showed a diffuse cytoplasmic distribution (Figure 3A, control). As previously described (Tai et al., 2004; Turjanski et al., 2007), ATP stimulation led to the nuclear redistribution of Erk2 (Figure 3A, +ATP). However, we observed that Erk2 also accumulated at the cell edges in local ruffling areas and at the base of some filopodia (Figure 3A, +ATP, arrows; Figure S3). When HeLa or HCx26 cells, transfected with GFP-Erk2, were challenged with wild-type *Shigella*, clusters of Erk2 were visualized at the base of NMEs interacting with bacteria (Figure 3B), suggesting a role for Erk1/2 in the control of the dynamics of NMEs. To investigate the role of Erk1/2 in NME-mediated bacterial capture, we treated cells with the Mitogen-activated protein kinase kinase (MEK) inhibitor U0126, which prevents Erk1/2 activation. Anti-phospho Erk1/2 western blot analysis indicated that cell treatment for 45 min in the presence of U0126 at a final concentration of 25 μM prevented ATP- and bacterial-induced Erk1/2 activation (data not shown). To determine whether Erk1/2 inhibition affected bacterial capture by NMEs, we incubated HeLa and HCx26 cells treated with U0126 with wild-type *Shigella*, the plasmid-cured isogenic strain BS176, or with the irrelevant *E. coli* K12 MC4100 and fixed them to quantify the number of bacteria interacting with NMEs. Cell treatment with U0126 did not prevent but, on the contrary, increased the capture of wild-type *Shigella* in HeLa and HCx26 cells but not that of BS176 or *E. coli* (Figure 3C). However, when real-time analysis of NME dynamics upon capture of *Shigella* was performed, U0126-treated cells were much less proficient at retracting NMEs after bacterial capture, with a 4-fold decrease in HCx26 cells, and a 5-fold decrease in retraction in the case of parental HeLa cells (Figure 3D). These results show that retraction of *Shigella* captured by NMEs requires Erk1/2 activity.

Erk1/2 Controls the Actin Retrograde Flow in Filopodia

Erk1/2 was reported to regulate the activity of myosin II by inducing indirect phosphorylation of the myosin light chain (Klemke et al., 1997; Mansfield et al., 2000). In our conditions, however, we could not detect any increase in phosphorylated MLC upon ATP stimulation (data not shown). Furthermore, when cells were incubated with blebbistatin, which prevents myosin II activation by MLCK (Figure S4), we could not detect any difference in the frequency of NME-mediated bacterial capture and retraction (0.8 ± 0.17) compared to untreated cells (0.77 ± 0.1), although at the concentrations used, cell division was inhibited. These results suggest that myosin II is not required for NME retraction.

We then investigated the role of Erk1/2 in the regulation of actin dynamics in filopodia. Actin monomers assemble at

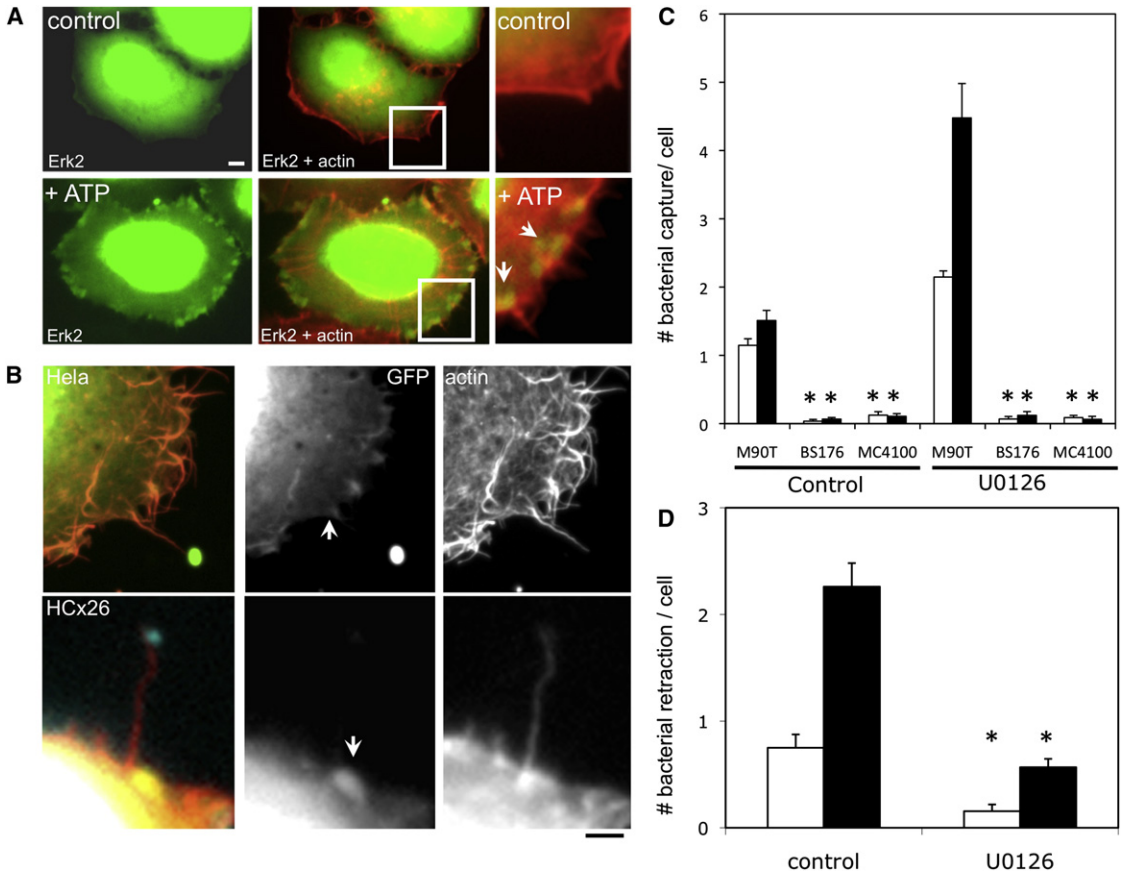

Figure 3. Erk1/2 Localizes at the Base of NME and Is Required for Their Retraction

(A) Extracellular ATP induces Erk2 localization at the base of filopodia. Representative fluorescence images of GFP-Erk2 (green) -transfected HeLa cells stimulated for 5 min with buffer alone (control) or with 50 μM ATP (+ATP). The right panels are magnification of the insets shown in the left panels. The scale bar represents 5 μm.

(B) Erk2 localizes at the base of NMEs during bacterial capture. Cells transfected with GFP-Erk2 were incubated with wild-type *Shigella* (HCx26 cells) or *Shigella* expressing GFP (HeLa cells) for 20 min, fixed, and processed for fluorescence staining. Blue, DAPI staining; red, rhodamine-phalloidin staining; green, GFP-Erk2 fluorescence. Top panels, HeLa cells; bottom panels, HCx26 cells. The scale bar represents 3 μm.

(C) Erk1/2 inhibition leads to increased bacterial capture by NMEs. Wild-type *Shigella*, BS176, or *E. Coli* MC4100 were incubated for 20 min with HeLa cells (white bars) or HCx26 cells (black bars) in the absence or in the presence of the MEK inhibitor U0126, and samples were fixed and processed for fluorescence staining of F-actin and bacteria (Experimental Procedures). The number of NME-mediated capture was scored by epifluorescence microscopy analysis. The average number of NME-mediated capture per cell was normalized over the value obtained for HeLa cells challenged in control conditions. Error bars correspond to the SEM (HeLa cells, n = 3, 142 cells; HCx26 cells, n = 3, 120 cells). *p < 0.0001.

(D) The U0126 inhibitor prevents NME retraction following bacterial capture. HeLa cells (white bars) or HCx26 cells (black bars) were challenged with invasive BS167 and NME-mediated capture and retraction was analyzed by time-lapse microscopy. Cells were challenged in the following: control, buffer alone; U0126, in the presence of 20 μM U0126. The average number of NME-mediated retraction per cell was normalized over the value obtained for HeLa cells challenged in control conditions. At least three independent sets of experiments were performed for the quantification; error bars correspond to the SEM (HeLa, 83 cells; HCx26, 97 cells). *p < 0.0001 when tested against the corresponding untreated sample.

See also Figure S3.

free barbed ends of actin filaments at filopodial tips, pushing backward the actin network, a process called retrograde flow (Small and Resch, 2005). To measure the rate of the retrograde flow in filopodia (see the Experimental Procedures), we performed FRAP experiments on GFP-actin transfected HeLa cells and analyzed fluorescence recovery in actin filaments on kymographs. The rate of actin retrograde flow was determined as the rate of extension of the recovered fluorescence between the photobleached area and the edge of the membrane (Experimental Procedures).

The average rate of actin retrograde flow inside filopodia was estimated at 21.9 ± 1.8 nm/s (Figures 4A and 4E). Addition of ATP at a final concentration of 100 μM led to a slight increase of the average rate of actin retrograde flow (27 ± 3.8 nm/s) that did not appear to significantly differ from the one measured in unstimulated cells (Figures 4C and 4E). When U0126 was added, the rate of actin retrograde flow dramatically decreased to 5.3 ± 0.7 nm/s, whereas addition of U0124, the inactive U0126 analog had no effect (Figures 4B and 4E). When ATP was added in the presence of U0126, this rate, estimated at 4.9 ± 0.8 nm/s, was

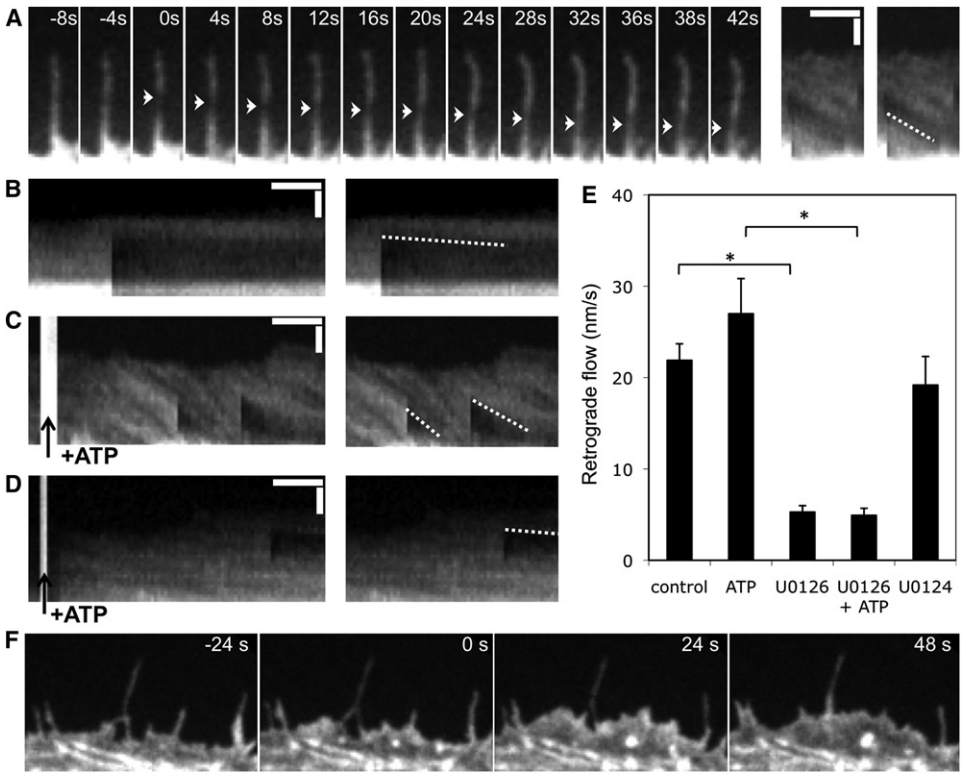

Figure 4. Erk1/2 Controls the Rate of Actin Retrograde Flow in Filopodia and Its ATP-Mediated Activation Transiently Induces Ruffles

(A) Measurement of actin retrograde flow in filopodia. HeLa cells transfected with GFP-actin were imaged with spinning-disk confocal microscopy every 4 s. Small areas in filopodia or in the cell cortex at their base were photobleached (arrowheads). Representative time-lapse recording of photobleached filopodia are shown in the left panels. Kymographs in filopodia were used to calculate the rate of actin retrograde flow from the photobleached tracks (right panels, dashed line). The vertical scale bar represents 1 μm and the horizontal scale bar 60 s.

(B) Erk1/2 controls the rate of actin retrograde flow. Kymographs analyze of FRAP experiments on filopodia of HeLa cells pre-incubated for 45 min in the presence of 25 μM U0126. The vertical scale bar represents 1 μm and the horizontal scale bar 60 s.

(C and D) Extracellular ATP leads to a slight increase in the rate of actin retrograde flow. Kymographs analyze of FRAP experiments on filopodia of HeLa cells preincubated for 45 min with buffer alone (C) or 25 μM U0126 (D) and treated with 100 μM ATP as indicated. The vertical scale bar represents 1 μm and the horizontal scale bar 60 s.

(E) The rate of actin retrograde flow in filopodia is controlled by Erk1/2. The average rates of actin filament assembly in filopodia derived from FRAP experiments are indicated ± SEM, before or after the addition of 100 μM ATP, in the absence or in the presence of 25 μM U0126 or U0124 (165 filopodia, 30 independent experiments, *$p < 0.000001$ when tested against the corresponding untreated sample).

(F) Extracellular ATP induces transient ruffles at the base of filopodia. Representative time-lapse recording of HeLa cells treated with ATP. 100 μM of ATP was added at time 0.

See also Figure S4 and Movies S3 and S4.

not further stimulated (Figures 4D and 4E). In addition, ATP treatment induced transient ruffles in the cortex, at the base of filopodia (Figure 4F and Movie S3). The formation of these ruffles was dependent on ATP-mediated Erk1/2 activation since they were not induced by ATP when cells were treated with U0126 (Movie S4). These data demonstrate that Erk1/2 activation controls the rate of actin retrograde flow in filopodia and the increased actin dynamics at their base in the cell cortex.

Filopodia Dynamics and Bacterial Capture by NME Require Actin Polymerization

To investigate the role of actin assembly in NME dynamics, we treated HeLa cells with cytochalasin D, which caps the barbed end of actin filaments at low concentrations but also sequesters monomers at high concentrations (Carlier et al., 1986). At high concentrations, all filopodial extensions disappeared, indicating that actin polymerization was required for NME formation (data not shown). However, at low concentrations of cytochalasin D, the numbers of extensions was reduced, concomitant with a decrease in their dynamics. In time-lapse acquisitions, filopodia were observed to elongate with an average rate of 8.2 ± 4.3 μm/min, reaching a maximum length that remained constant with an average half-life of 102 ± 37 s. Cytochalasin D increased the filopodial elongation rate to 13 ± 3.1 μm/min, as well as the filopodial half-life by 10-fold (1053 ± 260 s) (Figures 5A–5C and Movie S5). These long filopodia, however, were not proficient at capturing bacteria (Figure 5D). These data indicate that NME-mediated bacterial capture requires actin polymerization, possibly to stabilize contacts between the bacterium and the NME tip. The increased elongation rate of filopodia observed upon treatment with low concentrations of cytochalasin D is consistent with the proposed funneling effects of capping

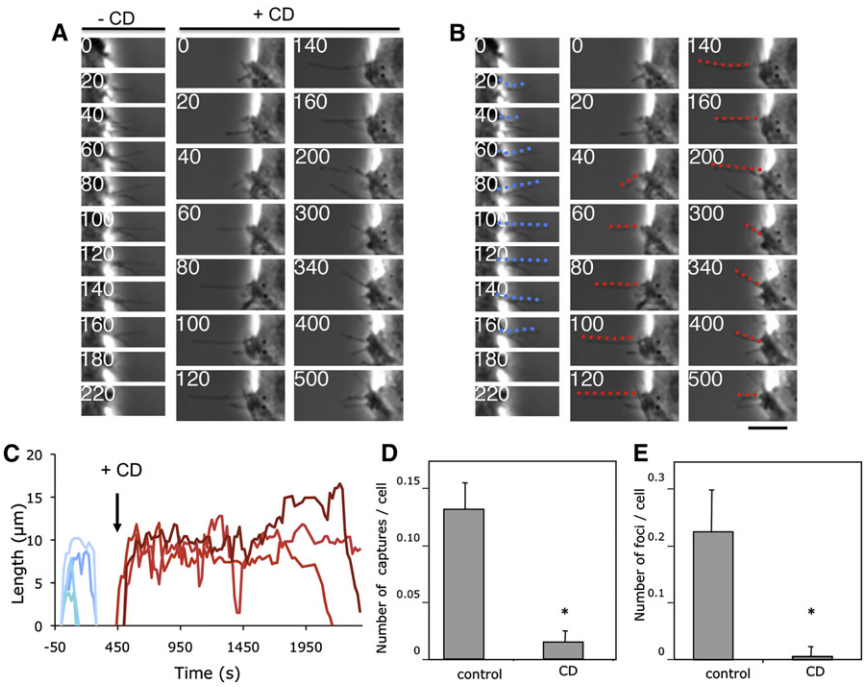

Figure 5. Baterial Capture and NME Dynamics Requires Actin Polymerization

(A–C) Cytochalasin D treatment affects filopodial dynamics. When indicated, cytochalasin D was added at 2 nM final concentration to HeLa cells, and samples were analyzed by phase-contrast microscopy. Representative time-lapse recordings of filopodia the absence (–CD) or in the presence of 2 nM cytochalasin D (+ CD) are shown in (A). In (B), the tracks used to measure filopodia lengths are represented with dashed lines. In (C), lengths of filopodia were quantified on time-lapse recording as in (B). The time following cytochalasin D addition is indicated in seconds. Filopodia are more stable after cytochalasin D treatment.

(D and E) Cytochalasin D inhibits *Shigella* capture by NMEs. HeLa cells were treated with 2 nM cytochalasin D for 15 min prior to challenge with the invasive *Shigella* BS167 strain at a MOI of 50 for 15 min. Samples were fixed and processed for phalloidin and DAPI staining. Samples were scored epifluorescence microscopy analysis. The average number of capture per cell is indicated ± SEM. (Control cells, n = 3, 1400 cells; cytochalasin D-treated cells, n = 3, 1260 cells.) NME capture/cell is shown in (D); *$p < 10^{-11}$ when tested against untreated sample. Bacterial-induced actin foci are shown in (E); *$p < 10^{-8}$ when tested against untreated sample. See also Movies S5 and S6.

proteins, where the capping of a fraction of the pool of actin filaments barbed ends leads to an increase in the concentration of monomeric actin, thereby favoring elongation of the remaining fraction of uncapped filaments (Pantaloni et al., 2001). The fact that cytochalasin D increased the stability of filopodia suggests that actin polymerization also controls filopodial retraction.

Erk1/2-Dependent NME Retraction Is Required for *Shigella* Invasion of Epithelial Cells

We then analyzed the effects of inhibiting Erk1/2 and NME retraction on bacterial invasion. Time-course analysis showed that cell treatment with U0126 led to a 33% to 38% inhibition of bacterial-induced actin foci in HCx26 cells and in parental HeLa cells (Figures 6A and 6B). This inhibition, however, was not observed when cell contact was forced by centrifugation or when adhesin-expressing bacteria were used, indicating that Erk1/2 was not required for invasion by bacteria already in contact with cell bodies (Figure 6C and Figure S5A).

To confirm the role of Erk1/2 and NME-mediated capture in wild-type *Shigella* invasion, we treated HeLa cells with short interfering RNA (siRNA) to knock down Erk1/2 expression (Figure 6D) and then tested them for their ability to internalize wild-type *Shigella* with a gentamicin protection assay (Tran Van Nhieu et al., 1997). As shown in Figure 6E, knockdown of Erk1/2 in HeLa cells resulted in a significant increase of filopodia length (5.1 ± 0.2 μm compared to 2.4 ± 0.1 μm for control cells, 243 filopodia analyzed, n = 2, $p < 0.00001$; Figure S5B), consistent with a role of Erk1/2 in NME retraction. Furthermore, the number of internalized bacteria was reduced to levels observed with the noninvasive *mxiD* strain (Figure 6F). Consistently, cell treatment with U0126 resulted in a reduced number of internalized bacteria, but this inhibition was not observed upon centrifugation of bacteria on cells (Figure S5C). These results indicate that Erk1/2 activity, which controls NME retraction, plays an important role for *Shigella* entry and support a role for NME-mediated capture in the early steps of bacterial invasion.

To test the role of NME-mediated capture in *Shigella* invasion of polarized colonic epithelial cells, we used Caco-2/TC7, which were allowed to polarize for 10 days prior to bacterial challenge (Experimental Procedures). As shown in Figure 7A, gentamicin protection assays indicated that invasion of wild-type *Shigella* was decreased by 2-fold in the presence of U0126. Immunofluorescence analysis was performed to visualize the early steps of bacterial invasion (Experimental Procedures). To increase bacterial adhesion to these cells in order to visualize bacterial-induced cytoskeletal reorganization during invasion, we used strains expressing the AfaE adhesin (Tran Van Nhieu et al., 1997). Although not as frequently observed as in nonpolarized HeLa cells, actin foci were detected at the apical face of Caco-2/TC7 cells challenged with invasive *Shigella*, but not with the noninvasive isogenic *mxiD* mutant (Figures 7B and 7C and data not shown). These entry foci occurred at the levels of cell-cell junctions and often implicated several bacteria (Figures 7B and 7C). In addition, and as shown in Figure 7C, bacterial interaction with NMEs were observed, emanating from *Shigella*-induced entry foci (yellow arrowheads) (Movies S6 and S7), suggesting that NME-mediated bacterial capture was responsible for the invasion of multiple bacterial at one entry site. Consistently, when cells were treated with U0126, the average number of bacteria associated with an entry site was decreased from 2.6 ± 0.16 in the absence of U0126 (93 foci, n = 2) to 1.8 ± 0.13 (82 foci, n = 2) in the presence of U0126 (Figure 7D).

These results suggest that NME-mediated capture favor invasion by increasing the amounts of bacteria invading per

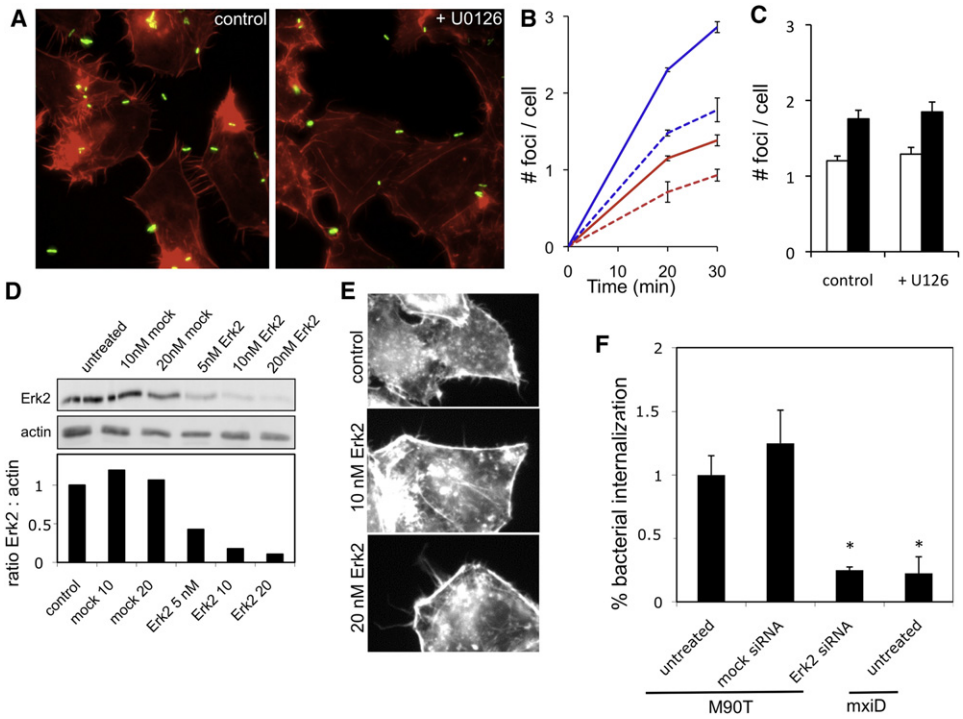

Figure 6. Inhibition of NME Retraction by Erk1/2 Inactivation Reduces *Shigella* Invasion

(A and B) A role for Erk1/2 in the early phases of *Shigella* invasion. HeLa cells (red curves) or HCx26 cells (blue curves) were challenged with invasive *Shigella* BS167 for the indicated time, in the absence (solid lines) or in the presence (dashed lines) of U0126. Samples were fixed, stained, and processed for F-actin staining. Representative images of *Shigella*-induced actin foci in HeLa cells after 20 min are shown in (A). The average number of foci per cell ± SEM is indicated in (B). U0126 reduces *Shigella*-induced actin foci formation by 36% at 20 min and 30 min, consistent with a role for Erk1/2 and NME retraction in bacterial invasion. (HeLa cells, n = 2, 1534 cells; HCx26 cells, n = 2, 1732 cells.)

(C) HeLa cells (white bars) or HCx26 cells (black bars) were challenged with the *Shigella* BS167-GFP strain in the absence or in the presence of 25 μM U0126 and centrifuged at 1000 g for 10 min at 20°C to force the contact between cells and bacteria. Samples were shifted to 37°C for 30 min, fixed, and processed for F-actin staining. (HeLa cells, n = 2, 181 cells; HCx26 cells, n = 2, 192 cells.)

(D) siRNA-mediated inhibition of Erk1/2 expression. HeLa cells were treated with 10 or 20 nM control siRNA or 5, 10, or 20 nM Erk2 siRNA as indicated, and cell lysates were analyzed by western blotting with anti-Erk2 (top) or anti-actin (middle) antibodies. The band intensities were quantified (Experimental Procedures), and the relative levels of Erk2 expression were normalized to actin levels (bottom panel).

(E) Erk1/2 knockdown results in increased filopodial length. Representative images of HeLa cells treated with 10 or 20 nM anti-Erk2 siRNA, fixed, and processed for fluorescence staining with Alexa546-phalloidin.

(F) Percentage of *Shigella* internalization in siRNA transfectants. HeLa cells treated with control siRNA or Erk2 siRNA were challenged with *Shigella* wild-type strain (M90T) or the noninvasive *mxiD* isogenic derivative for 45 min at 37°C. The percentage of internalized bacteria was quantified with the gentamicin protection assay (Tran Van Nhieu et al., 1997). Each value is the mean of three independent determinations ± SEM. *$p < 0.01$ when tested against cells challenged with the invasive *Shigella* strain M90T.

See also Figure S5.

entry foci, during the early stages of bacterial interaction with epithelial cells.

DISCUSSION

While investigating the basis for increased bacterial invasion in cells proficient for Cx- and ATP-mediated signaling, we found that during the early steps of *Shigella* invasion, bacteria are captured by NMEs that retract toward the cell body, where the invasion occurs. Extracellular ATP, which leads to an increase in bacterial invasion, simulates NME-mediated bacterial capture. Thus, NME retraction provides a functional mechanism that support increased *Shigella* invasion in Cx-expressing cells. We observed that extracellular ATP transiently stimulates the tyrosyl phosphorylation of Erk1/2, reminiscent of observations in neuronal growth cone filopodia (Gomez et al., 2001; Lakshmi and Joshi, 2006). Enhanced NME-mediated capture and retraction of *Shigella* in Cx-expressing cells is likely to be a consequence of the combination of increased dynamics of actin in NME and at the cell cortex at the NME's base that we observed upon ATP stimulation. Consistently, in other studies, ATP has been reported to stimulate membrane ruffles after G protein-coupled activation of purinergic receptors (Scott et al., 2006; Ohsawa et al., 2007). Alternatively, increased invasion could also result from an increase in the number of NMEs, an increase in their length, or an increase in the frequency of their retraction, mediated by Erk1/2 regulation of actin treadmilling.

In addition to its role in ATP-mediated stimulation of bacterial invasion, we show that Erk1/2 activity is required for filopodial retraction. Our FRAP experiments indicated that Erk1/2 controls

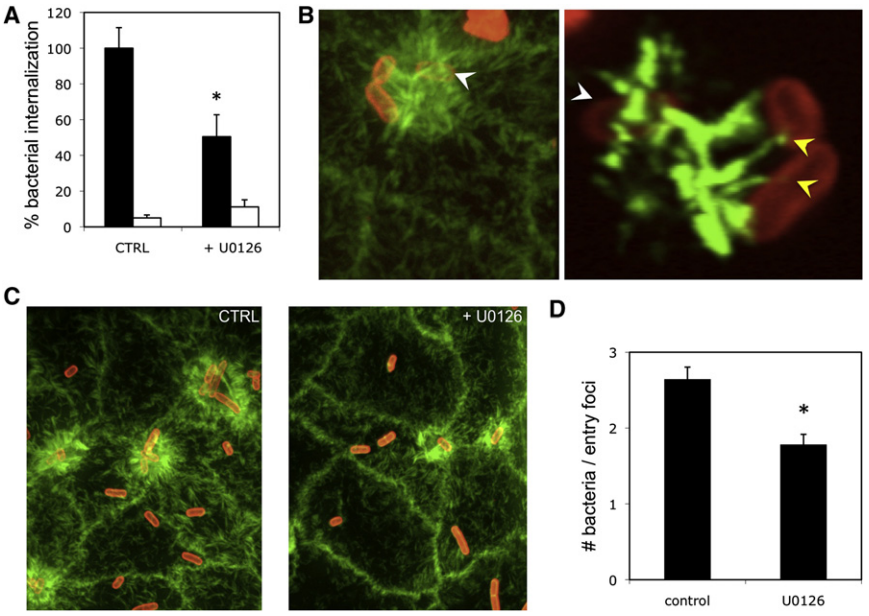

Figure 7. Invasion of Polarized Colonic Epithelial Cells through the Apical Side Is Dependent on Erk1/2

(A) Percentage of *Shigella* internalization upon U0126 treatment. Caco-2/TC7 cells, treated with or without 25 μM of U0126 as indicated, were challenged with *Shigella* wild-type strain (black bars) or the noninvasive *mxiD* isogenic derivative (white bars) for 15 min at 37°C. The percentage of internalized bacteria was quantitated with the gentamicin protection assay. Each value is the mean of three independent determinations ± SEM. *$p < 0.001$ when tested against untreated cells challenged with the invasive *Shigella* strain M90T.

(B) *Shigella* enters through the apical side of polarized Caco-2/TC7 cells. Caco-2/TC7 cells were allowed to polarize for 10 days. Cells were incubated with the M90T AfaE strain, fixed, and processed for immunostaining. Z sections (100 nm) were acquired via spinning-disk confocal microscopy. A representative entry site is shown. Left: 3D reconstruction using maximum intensity projection, displayed with an angle of 10°. Right: 3D reconstruction from deconvolved images displayed with a −170° angle. Red, anti-LPS immunostaining; green, alexa488-phalloidin staining; yellow arrowheads, bacteria captured by NMEs; white arrowhead, bacteria engulfed in the host cell cytoplasm.

(C and D) Effects of U0126 on the number of bacteria per entry site. Cells incubated with the M90T AfaE strain were fixed and processed for immunostaining, and 100 nm Z sections were acquired via spinning-disk confocal microscopy (C). Shown is a Z projection view of *Shigella*-induced actin foci, in the absence (left) or in the presence (right) of 25 μM U0126. Quantification of the average number of bacteria per entry foci ± SEM, in the absence (empty bar, 93 entry foci, n = 3) or in the presence (solid bar, 83 entry foci, n = 3) of 25 μM U0126 is shown in (D). *$p < 0.0001$ when tested against untreated cells challenged with the invasive *Shigella* strain M90T.

See also Movies S6 and S7.

the retrograde flow of actin in filopodia, suggesting that Erk1/2-mediated actin assembly plays a role in the retraction of NMEs. Since, Erk1/2 was localized at the base of filopodia, Erk1/2 may control the polymerization of actin filaments against the plasma membrane at the base of NMEs, which, if connected to the filopodial actin network, could act as a gear pulling the NME toward the cell body. Thus, NME retraction may be linked to differential rates of actin polymerization in NME and in the cell cortex, controlled by Erk1/2. The control of actin assembly by Erk1/2 could occur by the regulation of actin nucleation, filaments capping or disassembly, as previously reported (Martinez-Quiles et al., 2004; Menna et al., 2009; Nakanishi et al., 2007). In other systems, myosin motors walking toward the barbed ends of filopodial actin filaments participate in filopodial retraction (Faix and Rottner, 2006). While myosin II has been involved in virus gliding on filopodia and Erk1/2 was shown to regulate myosin light chain activation (Klemke et al., 1997; Mansfield et al., 2000; Lehmann et al., 2005), we could not detect myosin II activation upon extracellular ATP-mediated signaling. Furthermore, blebbistatin did not interfere with bacterial capture and NME retraction. These results suggest that myosin II is not required for NME retraction, although they do not rule out the potential implication of other myosins (Kerber et al., 2009; Les Erickson et al., 2003; Liu et al., 2008). The absence of a detectable role for myosin motors in the retraction of NME, which are not connected to the substrate as opposed to filopodia onto which viruses glide, is in line with the prominent role for Erk1/2 regulating actin assembly.

Filopodia have been described in various cell types as extensions that explore the cell environment, initiate contacts or transmit cell-to-cell signals (Faix and Rottner, 2006; Rørth, 2003). Various viruses invade cells by interacting with the side of filopodia and glide toward the cell body (Lehmann et al., 2005; Sowinski et al., 2008). *Yersinia* has been shown to adhere to filopodia prior to invasion in epithelial cells (Young et al., 1992), and filopodial capture was observed in macrophages phagocytosis of invasin-coated beads (Vonna et al., 2007). Capture of pathogenic microbes by filopodia may thus appear as a general feature involving various bacterial ligands. *Shigella* does not adhere strongly to cells, but we show during that the early stages of invasion, bacteria interact with NMEs through the tip complex proteins IpaB and IpaD. As opposed to the *Yersinia* invasion, which shows high affinity for β1-integrins (Isberg, 1991), the *Shigella* T3SS tip complex components do not promote strong adhesion. Upon *Shigella* capture, NMEs retract to bring bacteria in contact with the cell body, where invasion is initiated. If retraction and invasion does not ensue, however, because of the fragility of filopodia, the bacteria-NME interaction is likely to disrupt. These observations explain how *Shigella* triggers its interaction with host cells without showing constitutive cell binding activity. Also, during bacterial invasion, NMEs were found to emanate from entry foci and to capture additional bacteria, accounting for the accumulation of bacteria at a single entry site either in HeLa cells or in polarized Caco-2/TC7 colonic epithelial cells (Figures 1 and 7 and Movie S1), a process stimulated by ATP and connexin-mediated signaling. Bacterial

capture by filopodia may represent a "clever" strategy to invade cells without being exposed on the cell surface, thereby potentially limiting innate immune defense signals.

EXPERIMENTAL PROCEDURES

Antibodies and Reagents

The polyclonal antibodies anti-IpaB, -IpaD and -*S. flexneri* Flex5a LPS have been described previously (Ménard et al., 1993; Mounier et al., 1997). The 4G10 anti-phosphotyrosine monoclonal antibody was from Upstate Biotechnology, (Lake Placid, NY), the anti-Erk2 polyclonal antibody from Santa Cruz Biotechnology (catalog number sc-154), the anti-phospho-Erk1/2 polyclonal from Cell Signaling Technology (catalog number 9101S), the peroxidase-coupled and alkaline phosphatase-coupled anti-mouse IgG and anti-rabbit IgG antibodies from Jackson Immunoresearch (West Grove, PA), and rhodamine-coupled phalloidin, FITC-coupled anti-rabbit IgG, and ATP from SIGMA (St. Louis, MO). siRNA against Erk1/2 was from QIAGEN (catalog number 1022564) (Gorina et al., 2009).

Cell Lines, Bacterial Strains, Plasmids and Transfections

HeLa cells were obtained from the American Type Culture Collection and used between passages five and 15. HeLa transfectants expressing human connexin 26 (HCx26) and polarized colonic epithelial Caco-2/TC7 cells were described previously (Clair et al., 2008; Tran Van Nhieu et al., 2003). For these studies, two independent clones of HCx26, HCx26-1, and HCx26-2 were used (Tran Van Nhieu et al., 2003). Cells were grown in Dulbecco's modified Eagle's medium (DMEM, GIBCO) containing 10% fetal calf serum (FCS, GIBCO) for HeLa and HCx26 cells or 20% for Caco-2/TC7 with nonessential aminoacids, at 37°C in a 10% CO_2 incubator. The invasive *Shigella* rough LPS mutant strain of serotype 2a, BS167, its isogenic derivative cured from the virulence plasmid, BS169, the AfaE-expressing strain, and AfaE-M90T were described previously (Maurelli et al., 1985; Tran Van Nhieu et al., 1997). Bacterial strains were grown in trypticase soy (TCS) broth at 37°C with agitation. The pMW211 plasmid encoding DsRedS4T was described previously (Sörensen et al., 2003). The peGFPN1-Erk2 construct was kindly provided by Mark Scott (Institut Cochin, Paris, France). For transfection and siRNA treatment, cells were plated the day before at a density of 10^5 cells or 5×10^4 cells/25 mm coverslip (Marenfield), transfected with the jetPEI reagent (Polyplus Transfection) or the HiPerfect reagent (QIAGEN) according to the manufacturer's instructions, and incubated for 16 or 48 hr, respectively.

Quantification of NME-Mediated Bacterial Capture

HeLa cells (2×10^5) and HCx26 transfectants were plated the day before on glass coverslips. When indicated, cells were preincubated with 25 μM U0126 (Promega) for 30 min at 37°C in DMEM with 10% FCS. Samples were washed three times in EM buffer (120 mM NaCl, 7 mM KCl, 1.8 mM $CaCl_2$, 0.8 mM $MgCl_2$, 5 mM glucose, and 25 mM HEPES at pH 7.3), at room temperature. Bacteria grown until OD_{600} = 0.4 were washed three times in EM buffer and incubated when indicated with anti-IpaB or -IpaD or preimmune serum (1:10 dilution) for 5 min at room temperature prior to the addition to cells. Samples were shifted to 37°C for the indicated time, fixed in 3.7% paraformaldehyde for 1 hr at room temperature followed by overnight fixation at 4°C, and processed for F-actin staining with rhodamine-phalloidin and nuclear staining with DAPI (0.1 μg/ml). During the washing procedures, a pipette connected to a peristaltic pump (P1, GE Healthcare) was used at a flow rate of 10 ml/h^{-1} to avoid NME breakage.

Time-Lapse Phase-Contrast Microscopy Analysis

HeLa cells (2×10^5) or HCx26 transfectants were plated the day before on 25 mm diameter glass coverslips. Samples were rinsed three times in EM, mounted in a microscope chamber, and put in a 37°C temperature-controlled box for 10 min. They were challenged for 40 min with bacteria resuspended in EM buffer at a final A_{600} of 0.1 (MOI of 20) at 37°C. Wide-field microscopy analysis was performed with a LEICA DMRIBe inverted microscope (LEICA, Wetzlar, Germany) connected to a Cascade 512B camera (Roper's Instruments), driven by the Metamorph software (Universal Imaging). Images were acquired every 10 s and movies analyzed for quantification.

Immunofluorescence Analysis

For visualization of *Shigella*-induced actin foci, immunofluorescence staining was performed as described previously (Mounier et al., 1997; Tran Van Nhieu et al., 2003). HeLa cells (2×10^5) or HCx26 transfectants were plated the day before on glass coverslips. Cells were incubated with bacteria grown until OD_{600} = 0.4, at a MOI of 20, in EM buffer for 15 min at room temperature, or centrifuged at 1000 g for 10 min as indicated. For Caco-2/TC7 cells, 2×10^5 cells were plated on glass coverslips and allowed to grow to confluency and to polarize for 10 days. Cells were challenged with the bacteria in EM buffer (MOI = 300), shifted to 37°C for the indicated time periods, and immediately fixed with 3.7% paraformaldehyde. Samples were permeabilized in 0.1% Triton X-100 for 4 min, washed three times with PBS, blocked in DMEM containing 10% FCS for 15 min, and incubated with primary and secondary antibodies diluted as follows: rhodamine phalloidin (1:500) and anti-rabbit IgG coupled to Alexa525 or to Alexa470 secondary antibodies (1:200).

Gentamicin Protection Assay

The gentamicin protection assay was previously described, with minor modifications (Mounier et al., 1997). HeLa cells (10^5) plated the day before in 12-well plates were washed twice in PBS and challenged with bacteria in EM buffer containing 0.5% bovine serum albumin (MOI = 300) for 60 min at 37°C. When mentioned, samples were centrifuged at 2000 g for 10 min at 21°C. Samples were incubated in DMEM containing 10% FCS and 50 μg/ml gentamicin for 30 min at 37°C. Samples were then washed three times in PBS, lysed in 0.5% sodium deoxycholate, and plated onto agar plates for colony-forming unit counting. A similar procedure was used for Caco-2/TC7 cells, except that gentamicin treatment was performed in DMEM containing 20% FCS serum. When mentioned, cells were incubated with 25 μg/ml U0126 inhibitor in cell medium for 30 min at 37°C, prior to bacterial challenge.

Scanning Electron Microscopy

Bacteria were grown until OD_{600} = 0.4 and resuspended in DMEM containing 15 mM HEPES at pH 7.3. Cells were incubated with bacteria for the indicated times. Samples were washed in PBS, fixed overnight at 4°C in 2.5% glutaraldehyde in 0.1M cacodylate buffer (pH 7.2), washed three times for 5 min in 0.2 M cacodylate buffer (pH 7.2), postfixed for 1 hr in 1% osmium tetroxide in cacodylate buffer, and rinsed with distilled water. Samples were dehydrated through a graded series of 25%, 50%, 75%, and 95% ethanol solution in successive 5 min incubations and for 10 min in 100% ethanol followed by critical point drying with CO_2. Dried specimens were sputter coated twice with carbon with a BALTEC MED010 evaporator. Samples were analyzed with a JEOL JSM 6700F field emission scanning electron microscope operating at 5 Kv.

Western Blot Analysis

Cells were plated the day before at semiconfluency (5×10^5 cells in 35 mm culture dish), washed twice with PBS containing 1 mM sodium orthovanadate, challenged with bacteria grown at A_{600} = 1 for 5 min at room temperature, and incubated for the indicated times at 37°C or treated with the indicated concentrations of ATP at 37°C. Samples were transferred on ice, washed twice in ice-cold PBS containing sodium orthovanadate, and lysed in 200 μl Laemmli loading sample buffer. Samples were loaded onto SDS-PAGE gels and analyzed by anti-phosphotyrosine or anti-phosphoErk2 western blot. Filters were processed with ECL detection kit (Amersham) for phosphotyrosine or with Attophos (Promega) for anti-phospho Erk2 western blotting.

FRAP Experiments

HeLa cells (2×10^5) were plated on 25 mm diameter glass coverslips. After 24 hr, cells were transfected with GFP-actin and incubated at 37°C for 16 hr. Samples were rinsed three times in EM, mounted in a microscope chamber, put for 10 min, and observed at 37°C on an Eclipse Ti microscope (Nikon) equipped with a 100× objective (NA 1.4), a CSU-X1 spinning-disk confocal head (Yokogawa), an Evolve camera (Roper Scientific Instruments), and a FRAP module (Roper Scientific Instruments), controlled by the Metamorph 7.7 software. Images were acquired every 4 s for 10 min on a single plane with a 200 ms exposure time, and photobleached regions in the filopodia were determined during the acquisition.

SUPPLEMENTAL INFORMATION

Supplemental Information includes Supplemental Experimental Procedures, five figures, and seven movies and can be found with this article online at doi:10.1016/j.chom.2011.05.005.

ACKNOWLEDGMENTS

The authors thank Jost Enninga for his help and interest in these studies and Jérémie Teillon from the Centre de Recherche Interdisciplinaire en Biologie image analysis facility. This work was supported by the Institut National de la Santé et de la Recherche Médicale, the Institut Pasteur, the Institut National pour la Recherche Agronomique, the Collège de France, Agence Nationale pour la Recherche grants and National Institute of Health grant AI067949. P.J.S. is a Howard Hughes Medical Institute foreign scholar. S.R. received a fellowship from the Fondation pour la Recherche Médicale.

Received: January 19, 2011
Revised: April 19, 2011
Accepted: May 23, 2011
Published: June 15, 2011

REFERENCES

Carlier, M.F., Criquet, P., Pantaloni, D., and Korn, E.D. (1986). Interaction of cytochalasin D with actin filaments in the presence of ADP and ATP. J. Biol. Chem. *261*, 2041–2050.

Clair, C., Combettes, L., Pierre, F., Sansonetti, P., and Tran Van Nhieu, G. (2008). Extracellular-loop peptide antibodies reveal a predominant hemichannel organization of connexins in polarized intestinal cells. Exp. Cell Res. *314*, 1250–1265.

Cossart, P., and Sansonetti, P.J. (2004). Bacterial invasion: the paradigms of enteroinvasive pathogens. Science *304*, 242–248.

Faix, J., and Rottner, K. (2006). The making of filopodia. Curr. Opin. Cell Biol. *18*, 18–25.

Galán, J.E., and Wolf-Watz, H. (2006). Protein delivery into eukaryotic cells by type III secretion machines. Nature *444*, 567–573.

Garg, J.P., Chasan-Taber, S., Blair, A., Plone, M., Bommer, J., Raggi, P., and Chertow, G.M. (2005). Effects of sevelamer and calcium-based phosphate binders on uric acid concentrations in patients undergoing hemodialysis: a randomized clinical trial. Arthritis Rheum. *52*, 290–295.

Gomez, T.M., Robles, E., Poo, M., and Spitzer, N.C. (2001). Filopodial calcium transients promote substrate-dependent growth cone turning. Science *291*, 1983–1987.

Gorina, R., Santalucia, T., Petegnief, V., Ejarque-Ortiz, A., Saura, J., and Planas, A.M. (2009). Astrocytes are very sensitive to develop innate immune responses to lipid-carried short interfering RNA. Glia *57*, 93–107.

Guttman, J.A., Lin, A.E., Li, Y., Bechberger, J., Naus, C.C., Vogl, A.W., and Finlay, B.B. (2010). Gap junction hemichannels contribute to the generation of diarrhoea during infectious enteric disease. Gut *59*, 218–226.

Isberg, R.R. (1991). Discrimination between intracellular uptake and surface adhesion of bacterial pathogens. Science *252*, 934–938.

Kerber, M.L., Jacobs, D.T., Campagnola, L., Dunn, B.D., Yin, T., Sousa, A.D., Quintero, O.A., and Cheney, R.E. (2009). A novel form of motility in filopodia revealed by imaging myosin-X at the single-molecule level. Curr. Biol. *19*, 967–973.

Klemke, R.L., Cai, S., Giannini, A.L., Gallagher, P.J., de Lanerolle, P., and Cheresh, D.A. (1997). Regulation of cell motility by mitogen-activated protein kinase. J. Cell Biol. *137*, 481–492.

Lafont, F., Tran Van Nhieu, G., Hanada, K., Sansonetti, P., and van der Goot, F.G. (2002). Initial steps of Shigella infection depend on the cholesterol/sphingolipid raft-mediated CD44-IpaB interaction. EMBO J. *21*, 4449–4457.

Lakshmi, S., and Joshi, P.G. (2006). Activation of Src/kinase/phospholipase C/mitogen-activated protein kinase and induction of neurite expression by ATP, independent of nerve growth factor. Neuroscience *141*, 179–189.

Lehmann, M.J., Sherer, N.M., Marks, C.B., Pypaert, M., and Mothes, W. (2005). Actin- and myosin-driven movement of viruses along filopodia precedes their entry into cells. J. Cell Biol. *170*, 317–325.

Les Erickson, F., Corsa, A.C., Dose, A.C., and Burnside, B. (2003). Localization of a class III myosin to filopodia tips in transfected HeLa cells requires an actin-binding site in its tail domain. Mol. Biol. Cell *14*, 4173–4180.

Liu, R., Woolner, S., Johndrow, J.E., Metzger, D., Flores, A., and Parkhurst, S.M. (2008). Sisyphus, the Drosophila myosin XV homolog, traffics within filopodia transporting key sensory and adhesion cargos. Development *135*, 53–63.

Mansfield, P.J., Shayman, J.A., and Boxer, L.A. (2000). Regulation of polymorphonuclear leukocyte phagocytosis by myosin light chain kinase after activation of mitogen-activated protein kinase. Blood *95*, 2407–2412.

Martinez-Quiles, N., Ho, H.Y., Kirschner, M.W., Ramesh, N., and Geha, R.S. (2004). Erk/Src phosphorylation of cortactin acts as a switch on-switch off mechanism that controls its ability to activate N-WASP. Mol. Cell. Biol. *24*, 5269–5280.

Maurelli, A.T., Baudry, B., d'Hauteville, H., Hale, T.L., and Sansonetti, P.J. (1985). Cloning of plasmid DNA sequences involved in invasion of HeLa cells by Shigella flexneri. Infect. Immun. *49*, 164–171.

Ménard, R., Sansonetti, P.J., and Parsot, C. (1993). Nonpolar mutagenesis of the ipa genes defines IpaB, IpaC, and IpaD as effectors of Shigella flexneri entry into epithelial cells. J. Bacteriol. *175*, 5899–5906.

Menna, E., Disanza, A., Cagnoli, C., Schenk, U., Gelsomino, G., Frittoli, E., Hertzog, M., Offenhauser, N., Sawallisch, C., Kreienkamp, H.J., et al. (2009). Eps8 regulates axonal filopodia in hippocampal neurons in response to brain-derived neurotrophic factor (BDNF). PLoS Biol. *7*, e1000138.

Mounier, J., Bahrani, F.K., and Sansonetti, P.J. (1997). Secretion of Shigella flexneri Ipa invasins on contact with epithelial cells and subsequent entry of the bacterium into cells are growth stage dependent. Infect. Immun. *65*, 774–782.

Nakanishi, O., Suetsugu, S., Yamazaki, D., and Takenawa, T. (2007). Effect of WAVE2 phosphorylation on activation of the Arp2/3 complex. J. Biochem. *141*, 319–325.

Ogawa, M., Handa, Y., Ashida, H., Suzuki, M., and Sasakawa, C. (2008). The versatility of Shigella effectors. Nat. Rev. Microbiol. *6*, 11–16.

Ohsawa, K., Irino, Y., Nakamura, Y., Akazawa, C., Inoue, K., and Kohsaka, S. (2007). Involvement of P2X4 and P2Y12 receptors in ATP-induced microglial chemotaxis. Glia *55*, 604–616.

Pantaloni, D., Le Clainche, C., and Carlier, M.F. (2001). Mechanism of actin-based motility. Science *292*, 1502–1506.

Parsot, C., Ménard, R., Gounon, P., and Sansonetti, P.J. (1995). Enhanced secretion through the Shigella flexneri Mxi-Spa translocon leads to assembly of extracellular proteins into macromolecular structures. Mol. Microbiol. *16*, 291–300.

Phalipon, A., and Sansonetti, P.J. (2007). Shigella's ways of manipulating the host intestinal innate and adaptive immune system: a tool box for survival? Immunol. Cell Biol. *85*, 119–129.

Rørth, P. (2003). Communication by touch: role of cellular extensions in complex animals. Cell *112*, 595–598.

Saez, J.C., Berthoud, V.M., Branes, M.C., Martinez, A.D., and Beyer, E.C. (2003). Plasma membrane channels formed by connexins: their regulation and functions. Physiol. Rev. *83*, 1359–1400.

Scott, M.G., Pierotti, V., Storez, H., Lindberg, E., Thuret, A., Muntaner, O., Labbé-Jullié, C., Pitcher, J.A., and Marullo, S. (2006). Cooperative regulation of extracellular signal-regulated kinase activation and cell shape change by filamin A and beta-arrestins. Mol. Cell. Biol. *26*, 3432–3445.

Small, J.V., and Resch, G.P. (2005). The comings and goings of actin: coupling protrusion and retraction in cell motility. Curr. Opin. Cell Biol. *17*, 517–523.

Sörensen, M., Lippuner, C., Kaiser, T., Misslitz, A., Aebischer, T., and Bumann, D. (2003). Rapidly maturing red fluorescent protein variants with strongly enhanced brightness in bacteria. FEBS Lett. *552*, 110–114.

Sowinski, S., Jolly, C., Berninghausen, O., Purbhoo, M.A., Chauveau, A., Köhler, K., Oddos, S., Eissmann, P., Brodsky, F.M., Hopkins, C., et al. (2008).

Membrane nanotubes physically connect T cells over long distances presenting a novel route for HIV-1 transmission. Nat. Cell Biol. *10*, 211–219.

Spray, D.C., Ye, Z.C., and Ransom, B.R. (2006). Functional connexin "hemichannels": a critical appraisal. Glia *54*, 758–773.

Tai, C.J., Chang, S.J., Leung, P.C., and Tzeng, C.R. (2004). Adenosine 5′-triphosphate activates nuclear translocation of mitogen-activated protein kinases leading to the induction of early growth response 1 and raf expression in human granulosa-luteal cells. J. Clin. Endocrinol. Metab. *89*, 5189–5195.

Tran Van Nhieu, G., Ben-Ze'ev, A., and Sansonetti, P.J. (1997). Modulation of bacterial entry into epithelial cells by association between vinculin and the Shigella IpaA invasin. EMBO J. *16*, 2717–2729.

Tran Van Nhieu, G., Clair, C., Bruzzone, R., Mesnil, M., Sansonetti, P., and Combettes, L. (2003). Connexin-dependent inter-cellular communication increases invasion and dissemination of Shigella in epithelial cells. Nat. Cell Biol. *5*, 720–726.

Turjanski, A.G., Vaqué, J.P., and Gutkind, J.S. (2007). MAP kinases and the control of nuclear events. Oncogene *26*, 3240–3253.

Veenendaal, A.K., Hodgkinson, J.L., Schwarzer, L., Stabat, D., Zenk, S.F., and Blocker, A.J. (2007). The type III secretion system needle tip complex mediates host cell sensing and translocon insertion. Mol. Microbiol. *63*, 1719–1730.

Vonna, L., Wiedemann, A., Aepfelbacher, M., and Sackmann, E. (2007). Micromechanics of filopodia mediated capture of pathogens by macrophages. Eur. Biophys. J. *36*, 145–151.

Watarai, M., Kamata, Y., Kozaki, S., and Sasakawa, C. (1997). rho, a small GTP-binding protein, is essential for Shigella invasion of epithelial cells. J. Exp. Med. *185*, 281–292.

Willecke, K., Eiberger, J., Degen, J., Eckardt, D., Romualdi, A., Güldenagel, M., Deutsch, U., and Söhl, G. (2002). Structural and functional diversity of connexin genes in the mouse and human genome. Biol. Chem. *383*, 725–737.

Young, V.B., Falkow, S., and Schoolnik, G.K. (1992). The invasin protein of Yersinia enterocolitica: internalization of invasin-bearing bacteria by eukaryotic cells is associated with reorganization of the cytoskeleton. J. Cell Biol. *116*, 197–207.